

# Lawrence Berkeley National Laboratory

## Lawrence Berkeley National Laboratory

### **Title**

Neutron detection technique

### **Permalink**

<https://escholarship.org/uc/item/0xb195v9>

### **Authors**

Oblath, N.S.

Poon, A.W.P.

### **Publication Date**

2000-09-14

# Neutron Detection Technique

N. S. Oblath, A. W. P. Poon

*Lawrence Berkeley National Laboratory, Berkeley, CA 94720*

August 11, 2000

## **Abstract**

The Sudbury Neutrino Observatory (SNO) has the ability to measure the total flux of all active flavors of neutrinos using the neutral current reaction, whose signature is a neutron. By comparing the rates of the neutral current reaction to the charged current reaction, which only detects electron neutrinos, one can test the neutrino oscillation hypothesis independent of solar models. It is necessary to understand the neutron detection efficiency of the detector to make use of the neutral current reaction. This report demonstrates a coincidence technique to identify neutrons emitted from the  $^{252}\text{Cf}$  neutron calibration source. The source releases on average four neutrons when a  $^{252}\text{Cf}$  nucleus spontaneously fissions. Each neutron is detected as a separate event when the neutron is captured by a deuteron, releasing a gamma ray of approximately 6.25 MeV. This gamma ray is in turn detected by the photomultiplier tube (PMT) array. By investigating the time and spatial separation between neutron-like events, it is possible to obtain a pure sample of neutrons for calibration study. Preliminary results of the technique applied to two calibration runs are presented.

## **Disclaimer**

These data have been taken by the SNO collaboration as a whole, but have been analyzed entirely by the author. The presentation, results and conclusions have neither been approved nor disapproved by the SNO collaboration and do not necessarily represent the views of the collaboration.

# Contents

<b>1</b>	<b>Introduction</b>	<b>5</b>
1.1	The Sudbury Neutrino Observatory . . . . .	5
1.2	The Neutral Current Reaction . . . . .	5
1.3	$^{252}\text{Cf}$ Calibration Source . . . . .	6
<b>2</b>	<b>Basic Strategy of Neutron Analysis</b>	<b>6</b>
<b>3</b>	<b>Nhits Correlation Study</b>	<b>8</b>
3.1	Nhits <sub>0</sub> -Nhits <sub>1-5</sub> Correlation Regions . . . . .	8
3.2	$R_{fit}$ Cuts to Select the Neutron Sample . . . . .	10
3.3	Systematics of Nhits <sub>1-5</sub> Cuts . . . . .	10
<b>4</b>	<b>Systematics of the <math>R_{fit}</math> Cut</b>	<b>14</b>
<b>5</b>	<b>The Purified Neutron Sample</b>	<b>14</b>
5.1	Applying FiST . . . . .	14
5.2	$\Delta t$ of the Purified Sample . . . . .	17
<b>6</b>	<b>Conclusions</b>	<b>17</b>
<b>7</b>	<b>Acknowledgements</b>	<b>20</b>

# List of Figures

1	Raw Nhits spectrum, Run 11841 . . . . .	7
2	Nhits <sub>0</sub> -Nhits <sub>1</sub> correlation . . . . .	9
3	Nhits <sub>0</sub> and Nhits <sub>1</sub> distributions for different R <sub>fit0</sub> and R <sub>fit1</sub> cuts . . . . .	11
4	Nhits <sub>0</sub> and Nhits <sub>1-3</sub> distributions for R <sub>fit0</sub> <3m and R <sub>fit1-3</sub> <3m . . . . .	12
5	Nhits <sub>0</sub> and Nhits <sub>4-5</sub> distributions for R <sub>fit0</sub> <3m and R <sub>fit4-5</sub> <3m . . . . .	13
6	Nhits <sub>0</sub> distributions for different Nhits <sub>1</sub> cuts . . . . .	15
7	R <sub>fit0</sub> vs Nhits <sub>0</sub> . . . . .	16
8	Applying FiST to the Purified Neutron Sample . . . . .	18
9	$\Delta t$ of the Purified Neutron Sample . . . . .	19

## List of Tables

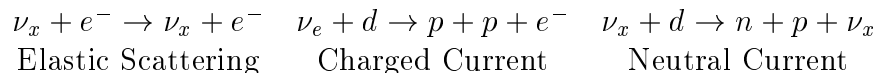
1	Neutrino reactions in SNO . . . . .	5
2	Event characterization in different regions of the $N_{\text{hits}_0}$ - $N_{\text{hits}_1}$ correlation plot.	8

# 1 Introduction

## 1.1 The Sudbury Neutrino Observatory

The Sudbury Neutrino Observatory (SNO) is a heavy water Cherenkov neutrino detector. It is located 2,000 meters underground in an active nickel mine near Sudbury, Ontario, Canada. SNO is unique in its use of 1,000 tonnes of heavy water to detect all three flavors of neutrinos. The neutrinos can react with the heavy water ( $D_2O$ ) in three different channels: Elastic Scattering (ES), Charged Current (CC) and Neutral Current (NC). The reactions are shown in Table 1.

Table 1: Neutrino reactions in SNO



The first two reactions produce a high energy electron. This electron produces a cone of light known as Cherenkov radiation which is detected by the 9,438 photomultiplier tubes (PMTs) which surround the heavy water. The neutral current reaction produces a neutron which can be detected in three different ways in the SNO detector. It can be captured by a deuteron in the heavy water, which releases a detectable gamma ray, or it can be detected through one of the enhanced detection methods. One such method is to dissolve salt in the  $D_2O$ . The neutrons are captured by the  $^{35}Cl$  nuclei, and a cascade of gamma rays is released. The other method is to use columns of  $^3He$  proportional counters anchored in an array throughout the  $D_2O$  volume. When the neutron is captured by the  $^3He$ , a proton and a triton are released. The proton and triton are detected in the proportional counters.

## 1.2 The Neutral Current Reaction

The Neutral Current reaction (NC) can detect the total flux of all three flavors of neutrinos, though it cannot distinguish between them. However, it is only with the NC reaction that SNO is able to test the hypothesis of neutrino oscillations independently of solar models. This can be done by comparing the number of neutrinos detected by the CC reaction, which are only electron neutrinos, to the number of neutrinos detected by the ES and NC reactions. Although the ES reaction is sensitive to  $\nu_\mu$  and  $\nu_\tau$ , the cross section to detect them is only about  $\frac{1}{6}$  that of  $\nu_e$ . Coupled with the fact that the ES detection rate is low in SNO, the NC measurement is much more powerful technique in measuring the total flux of all active neutrinos.

The signature of the NC reaction is a neutron. Out of the three particles in the final state, it is the only one that is detectable. When not using one of the enhanced neutron detection methods, the neutron is captured by a deuteron, releasing a 6.25 MeV gamma ray.

It is this gamma ray which must be detected. To correctly analyze the NC signal, one must first understand the neutron detection efficiency. The  $^{252}\text{Cf}$  source is used for this purpose.

### 1.3 $^{252}\text{Cf}$ Calibration Source

When a  $^{252}\text{Cf}$  nucleus spontaneously fissions, it emits on average 4 neutrons and approximately 20 low energy gamma rays. These fission neutrons are used to calibrate the neutron detection efficiency in SNO. The source is an acrylic cylinder with  $^{252}\text{Cf}$  in the center. The low energy gamma rays Compton scatter off of electrons in the  $\text{D}_2\text{O}$ , though most of them are below the Cherenkov threshold. The neutrons, however, wander for a short period of time until they are captured by a deuteron or by a hydrogen nucleus within the acrylic of the source, the heavy water <sup>1</sup> or the acrylic vessel. When a neutron is captured by a deuteron, a 6.25 MeV gamma ray is released, which Compton scatters off of an electron. This electron produces a cone of Cherenkov light which is detected by the PMTs.

## 2 Basic Strategy of Neutron Analysis

Since the low energy gamma rays produced by the  $^{252}\text{Cf}$  source are sometimes too weak to be detected or differentiated from the background, the key to identifying neutrons is to identify neutron coincidences from a fission event. Each neutron, when it captures on a deuteron, appears as a separate event in the SNO data stream.

The runs used in this analysis include Runs 11840 and 11841, each of which was approximately one hour long. The detector trigger rate due to the  $^{252}\text{Cf}$  source was  $\sim 1$  Hz. For both of these runs, the  $^{252}\text{Cf}$  calibration source was located at the center of the detector. For parts of the analysis, the two runs were combined to improve the statistics, which became quite low as more cuts were applied.

Figure 1 shows the raw Nhits (number of PMT hits) spectrum of Run 11841. The first peak contains low Nhit events which have integrated (over the entire detector) PMT signals of greater than approximately 150 photoelectrons (Energy Sum trigger). The second peak contains  $\beta\gamma$  events, which are signals from the decay of naturally occurring uranium and thorium, as well as low energy gamma events from neutrons captured on hydrogen nuclei in the acrylic of the source capsule, the  $\text{D}_2\text{O}$  and the acrylic vessel.

The third, broader peak contains the gamma rays from neutron capture on deuterium. The goal is to filter out the events which make up the majority of the first two peaks, leaving as many neutron events as possible. To do so we looked for neutron-neutron coincidence. In scanning through the data stream, we compared each event, called the “current event,” with the five “previous events” which came before it in the data. We examined the relationship between the current and previous events’ Nhit spectra and  $R_{fit}$  distributions. By making cuts on these two characteristics, a pure sample of neutrons from neutron-neutron coincidence can be selected.

---

<sup>1</sup>The heavy water in SNO has a D isotropic purity of 99.92%

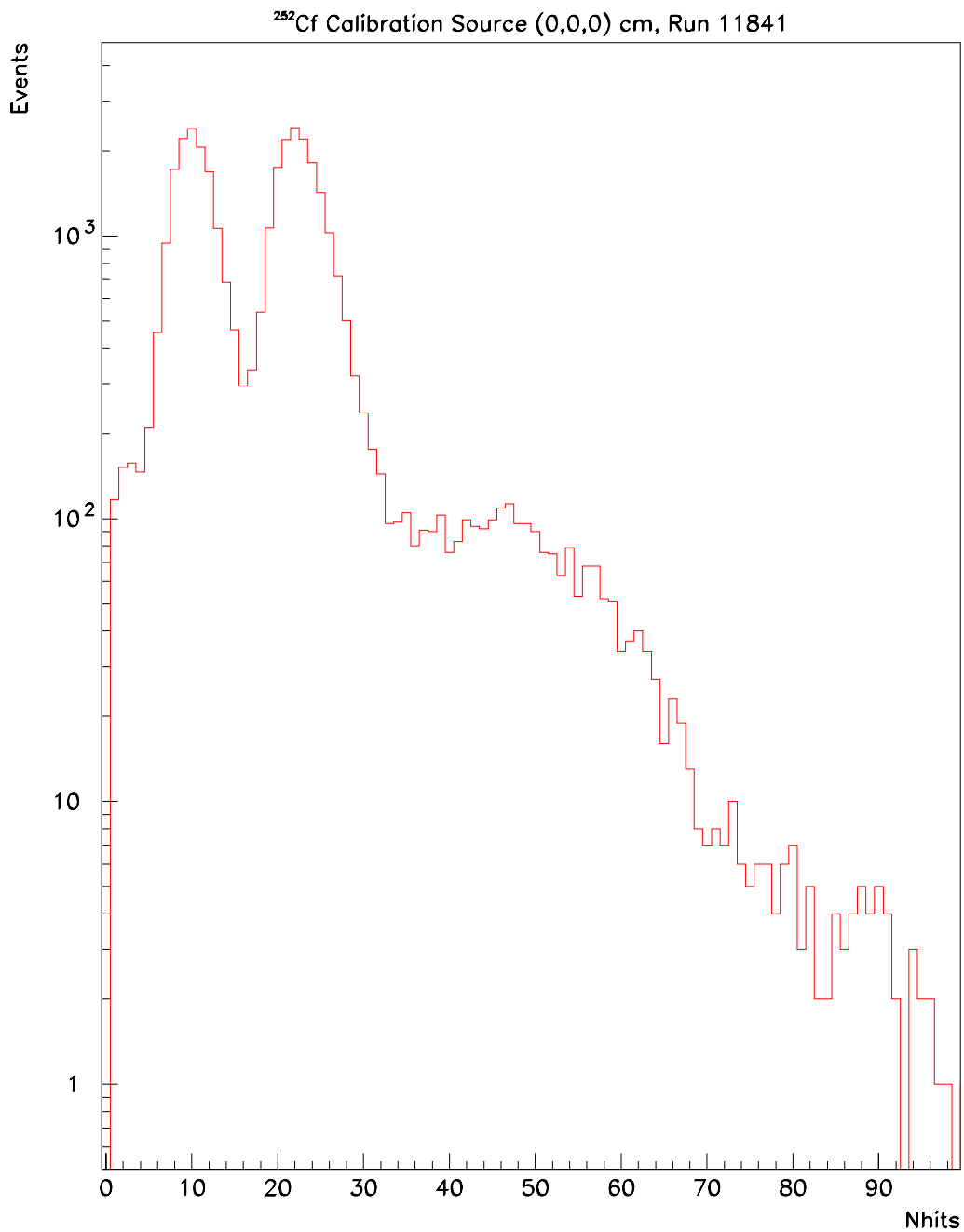


Figure 1: Raw Nhits spectrum for Run 11841. The first peak contains ESUM trigger events. The second peak contains  $\beta\gamma$  events and low energy gamma events. The third, broader peak contains the gamma events from neutrons captured on deuterium. In this run, the <sup>252</sup>Cf source was deployed in the center of the detector.



### 3 Nhits Correlation Study

#### 3.1 Nhits<sub>0</sub>-Nhits<sub>1-5</sub> Correlation Regions

A typical neutron capture on deuterium event involves between 30 and 70 PMT hits. We compared the Nhits of the current event (Nhits<sub>0</sub>) to the Nhits of the five events which preceded it (Nhits<sub>1</sub>, Nhits<sub>2</sub>,... Nhits<sub>5</sub>). Figure 2 is a scatter plot of Nhits<sub>0</sub> against the Nhits<sub>1</sub>. For the most part, the data points fall within the five regions that are marked in the plot.

Based on the Nhits values within each region, and knowing the characteristics of different varieties of events, we can qualitatively determine what types of event pairs populate each region. Table 2 lists each region, and the types of events which make up the majority of the data points within them. The background events come from a variety of sources, though they are significantly made up of uranium and thorium decays. Though great efforts were made to keep the contamination levels low in the materials that went into constructing SNO, a certain level of residual contamination remains, and produces a low energy background signal. The gamma events are the low energy gamma rays from the <sup>252</sup>Cf spontaneous fission or neutron capture by hydrogen. As can be seen in Figure 2, they can be difficult to distinguish from background events, so they cannot be used to tag neutron events.

Table 2: Event characterization in different regions of the Nhits<sub>0</sub>-Nhits<sub>1</sub> correlation plot.

Region	Types of Event Pairs (Nhits <sub>1</sub> -Nhits <sub>0</sub> )
1	background-gamma
2	gamma-background, gamma-gamma
3	background-neutron, gamma-neutron
4	gamma-neutron, background-neutron
5	neutron-neutron

There are very few data points below 16 Nhits on the Nhits<sub>0</sub> axis because a cut on the reconstructed vertex of the current event ( $R_{fit0}$ ) was used to restrict the events to within 6 meters of the source position. This cut eliminated the  $\beta\gamma$  events from the PMTs which reconstructed beyond the acrylic vessel.

Even though the regions appear fairly well defined in Figure 2, There are tails to the neutron-neutron event pair peak which extend outside of region 5. Therefore a cut Nhits<sub>0</sub> or Nhits<sub>1-5</sub> cannot be made too strict, or too many neutron-neutron event pairs will be cut out, or too loose, which would allow more background and low energy gamma events into the sample.

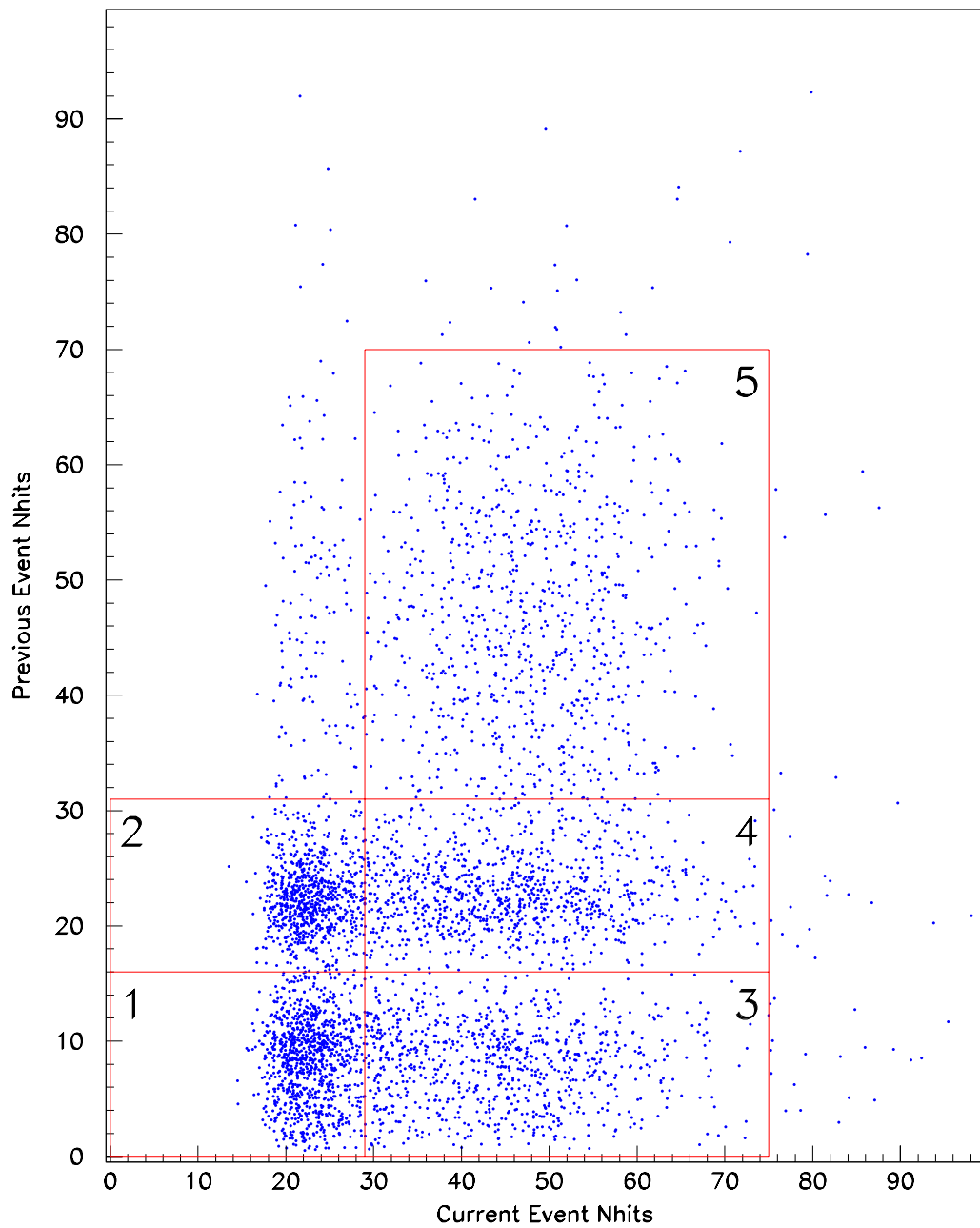


Figure 2: This plot shows  $N_{hits_0}$  plotted against  $N_{hits_1}$  from Run 11840. There are five main regions of data points. The neutron-neutron event pairs are mainly in region 5.

### 3.2 $R_{fit}$ Cuts to Select the Neutron Sample

To further improve the purity of the neutron sample, we placed cuts on the reconstructed vertices of the current and previous events. In addition to the 6 meter cut used in Figure 2, we placed a 3 meter cut on  $R_{fit1-5}$  and tightened the cut on  $R_{fit0}$  to 3 meters. Figure 3 shows the effect of these additional cuts on Nhits distributions of the previous and current events. The left column shows the  $Nhits_1$  and the right column shows  $Nhits_0$ . Each row of plots have different  $R_{fit}$  cuts used on the data. The first row has only a 6 meter cut on  $R_{fit0}$ . The two plots are they y and x projections of Figure 2. The second row has an additional 3 meter cut on  $R_{fit1}$ . The third row has a further restricted  $R_{fit0}$  cut, at 3 meters.

The largest decrease in the higher Nhits neutron peak is seen when the 3 meter  $R_{fit1}$  cut is imposed on the data. The peak drops from around 200 events/bin to approximately 80 events/bin. Looking at the  $Nhits_1$  spectra, most of the events that are removed with the 3 meter cut come from the two peaks around 10 and 25 Nhits. These events include ESUM trigger and low energy  $\gamma$  and  $\beta\gamma$  events. The low Nhits ESUM trigger events tend to fail the reconstruction or are reconstructed outside of the acrylic sphere because of the lack of Nhits. The  $\beta\gamma$  events are the result of the decays of naturally occurring uranium and thorium in the PMT array, and are therefore reconstructed to around 9 meters. Since there was already a 6 meter  $R_{fit0}$  cut, most of the ESUM trigger and low energy  $\gamma$  and  $\beta\gamma$  events had already been removed before the  $R_{fit0}$  cut was restricted to 3 meters. For that reason, there is not a large change in the Nhits spectra between the second and third pairs of plots in Figure 3. However, restricting the  $R_{fit0}$  cut to 3 meters does lower the low energy background peak that can be seen at approximately 25 Nhits.

Figures 4 and 5 show the differences in the Nhits spectra when looking for coincidences further back in time (i.e. the first through fifth previous events) to the current event. The cuts used to filter the events include a 3 meter  $R_{fit0}$  and  $R_{fit1-5}$  cuts. The neutron peak, at around 47 Nhits, becomes progressively worse compared to the residual background peak. For the first three pairs of plots, the neutron peak in the current event Nhits plots remains fairly distinct. For the fourth and fifth previous event Nhits, the current event Nhits neutron peak becomes even with the lower energy background peak. This shows that most of the useful neutron-neutron pairs will fall within three events of each other. However, in the analysis, the timing between the events has not been investigated. Including the difference in time between the events should allow one to further purify the neutron peaks.

### 3.3 Systematics of $Nhits_{1-5}$ Cuts

In Figure 4, the background peak at about 25 Nhits in the previous event Nhits spectra is clearly significant compared to the neutron event peak. Even with the  $R_{fit}$  cuts, a large number of background in the previous events sample still remain in the neutron sample. This means that the sample is not purely neutron-neutron event pairs. By using an  $Nhits_{1-5}$  threshold cut, we could eliminate a large number of the background previous events, while leaving most of the neutron previous events intact. We tested four different  $Nhits_{1-5}$  cuts, and examined their effect on the  $Nhits_0$  spectrum, to determine where, approximately, we

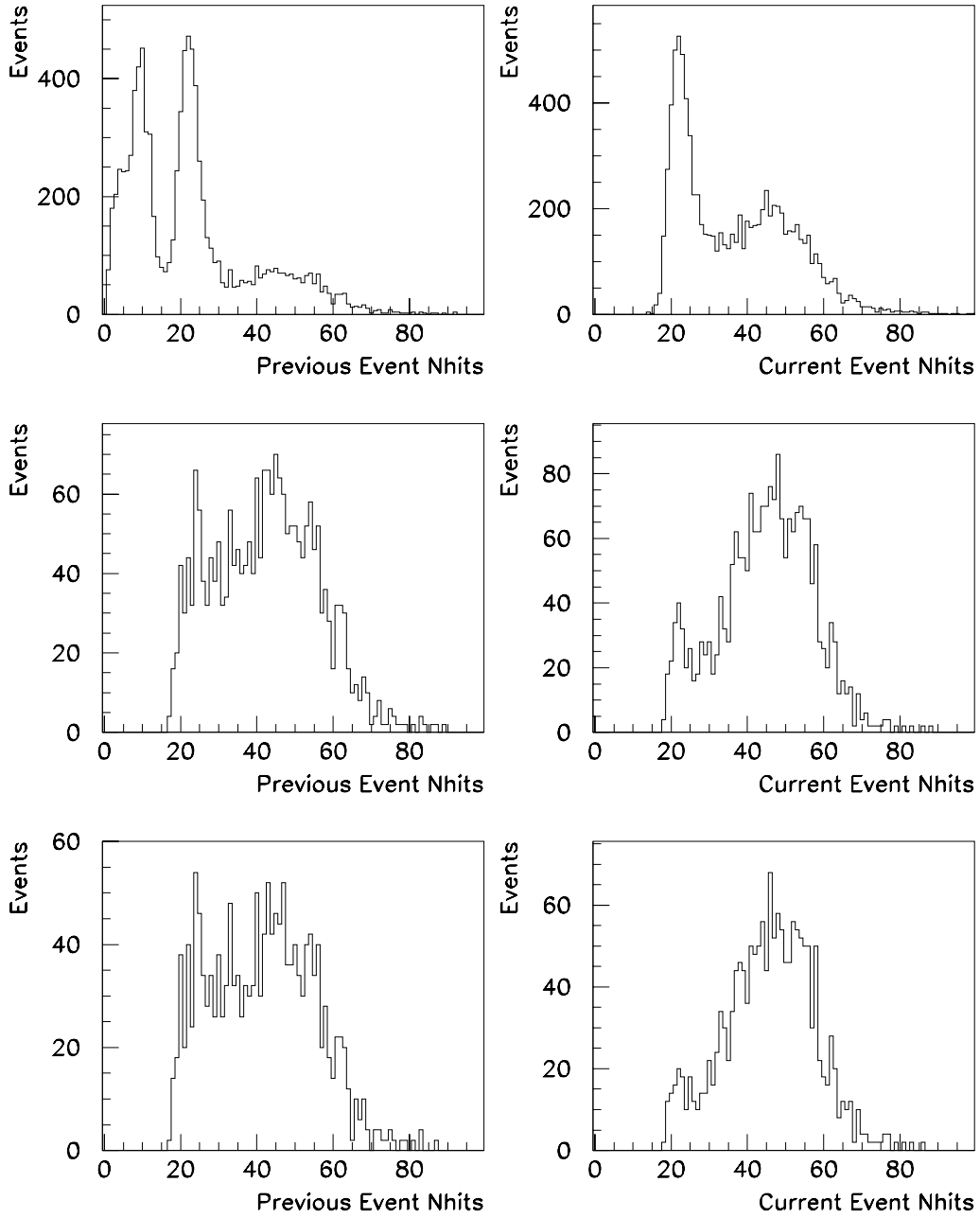


Figure 3: For each pair, the plot on the left is the  $N_{hits_1}$  spectrum, and the plot on the right is the  $N_{hits_0}$  spectrum. The first row have only a 6 meter  $R_{fit0}$  cut. The second row have an additional 3 meter  $R_{fit1}$  cut. The third row have a 3 meter  $R_{fit0}$  and  $R_{fit1}$  cuts. Events from Runs 11840 and 11841 are included in these plots.

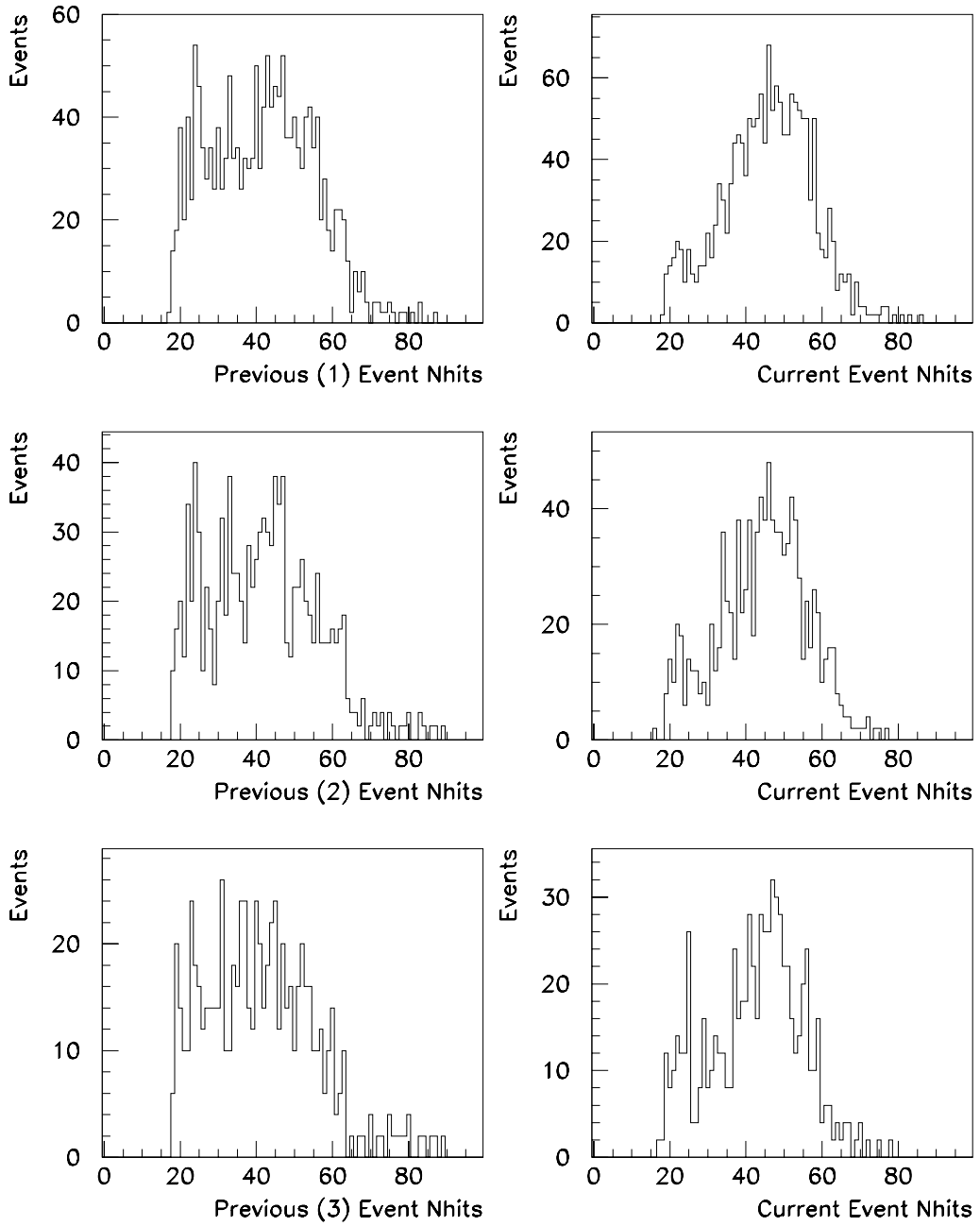


Figure 4:  $N_{hits_0}$  and  $N_{hits_{1-3}}$  distributions for the first through third previous events in Runs 11840 and 11841. The cuts used on these plots include 3 meter  $R_{fit0}$  and  $R_{fit1-3}$  cuts.

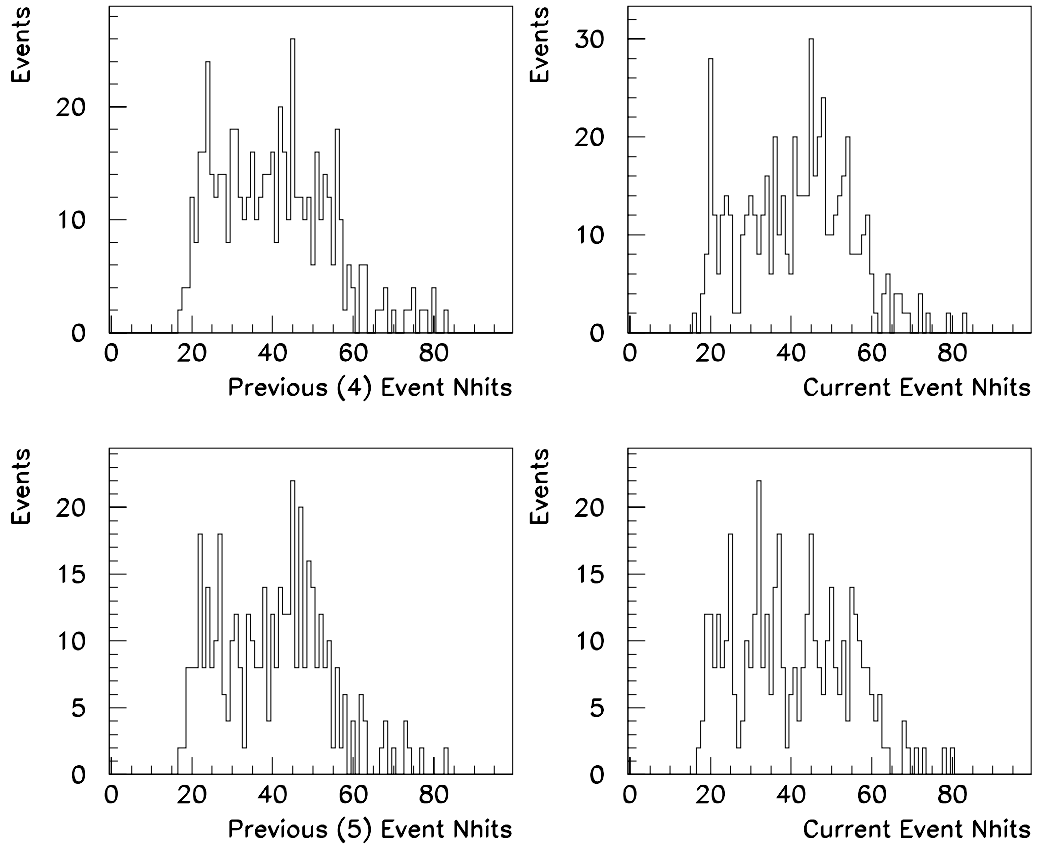


Figure 5:  $N_{hits_0}$  and  $N_{hits_{4-5}}$  distributions for the fourth and fifth previous events in Runs 11840 and 11841. The cuts used on these plots include 3 meter  $R_{fit_0}$  and  $R_{fit_{4-5}}$  cuts.

should set the  $N_{hits_{1-5}}$  cut so as to purify the sample as much as possible while still leaving most of the neutron-neutron event pairs in the sample. Figure 6 shows the  $N_{hits_0}$  spectra for the four different  $N_{hits_1}$  threshold cuts: 25, 30, 35 and 40. These cuts were made in addition to the  $R_{fit}$  cuts discussed above.

The  $N_{hits}$  peak agrees with Monte Carlo and  $^{16}N$  data, which is a 6.13 MeV  $\gamma$ -ray source. The  $N_{hits_1} > 25$  and 30 cuts seem to reduce the background while not reducing the neutron peak very much. Using  $N_{hits_1} > 35$  and 40 cuts, however, more drastically reduces the number of neutron events that are selected without significantly reducing the number of background events. To determine exactly where the  $N_{hit_{1-5}}$  cut should be made, it will be necessary to study more closely what percentage of neutron and background events are discarded with different  $N_{hits}$  cuts.

## 4 Systematics of the $R_{fit}$ Cut

The selection of 3 meters for the  $R_{fit}$  cuts used above was made somewhat arbitrarily. It was based on an estimate of how far the neutrons from the  $^{252}Cf$  source might wander before being captured by a deuteron. It was useful for the purpose of seeing the effect of  $R_{fit0}$  and  $R_{fit_{1-5}}$  cuts. However, to determine a more ideal  $R_{fit}$  cut, we compared the  $R_{fit0}$  distribution to the  $N_{hit_0}$  spectrum. Figure 7 shows a scatter plot of the reconstructed vertex with the  $N_{hits}$ , for each event. The  $R_{fit0}$  cut was removed, though the  $R_{fit1}$  cut and a  $N_{hit_1} > 30$  cut were retained.

As can be seen in Figure 7, the majority of the low  $N_{hit}$  events, centered around 25  $N_{hits}$ , are reconstructed to between 9 and 10 meters from the source position. Most of the neutron events, on the other hand, are between 0 and 4 meters. The histogram in Figure 8 without data cleaning shows the  $N_{hits_0}$  distribution with 4 meter  $R_{fit0}$  and  $R_{fit1}$  cuts, as well as a 30  $N_{hit_1}$  threshold cut. The neutron sample has very little background, though it will necessary to study the  $R_{fit0}$  and  $R_{fit_{1-5}}$  distributions to determine the most efficient combination of  $R_{fit}$  and  $N_{hits}$  cuts.

## 5 The Purified Neutron Sample

### 5.1 Applying FiST

Up to this point we had performed our analysis without using data cleaning cuts. Since the work was aimed at calibrating the detector, using data cleaning would have complicated the work, altering the event coincidence by removing events and changing the systematic uncertainties.

With the goal of testing the purity of the neutron sample, we applied the FiST data cleaning cuts to the sample after making the  $N_{hits_1}$  and  $R_{fit_{0,1}}$  cuts. This allowed us to determine how much of the neutron sample was composed of background events. We applied two FiST masks, with and without the Burst cut (DARN masks 0xB3B07 and 0xB3B06

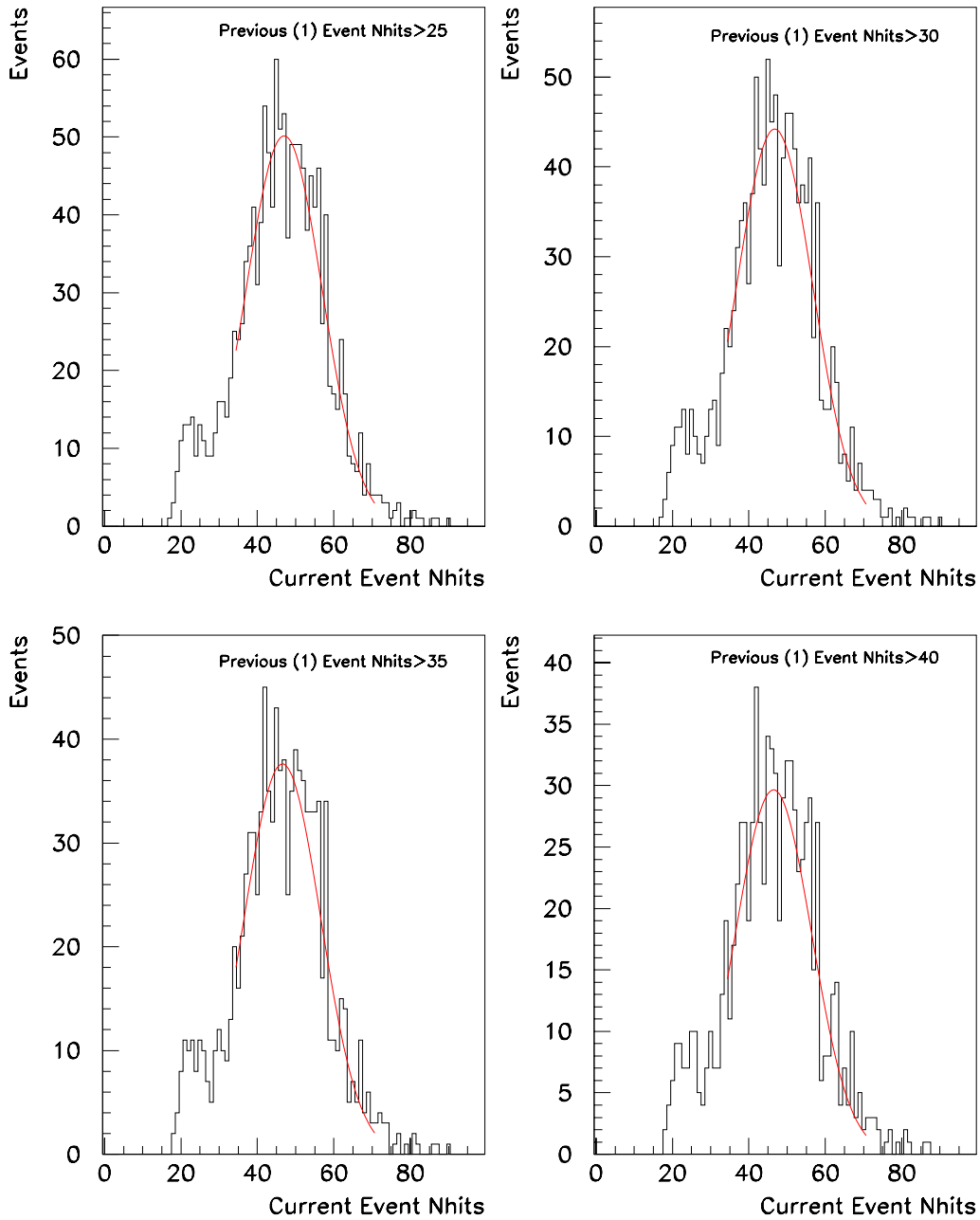


Figure 6: Four different  $N_{hits_1}$  cuts were used to attempt to further filter the event pair sample: 25, 30, 35 and 40 Nhits. These plots include data from Runs 11840 and 11841. Each histogram was fitted to a gaussian. The centroid of the gaussians agrees with Monte Carlo expectations for neutron capture on deuterium.



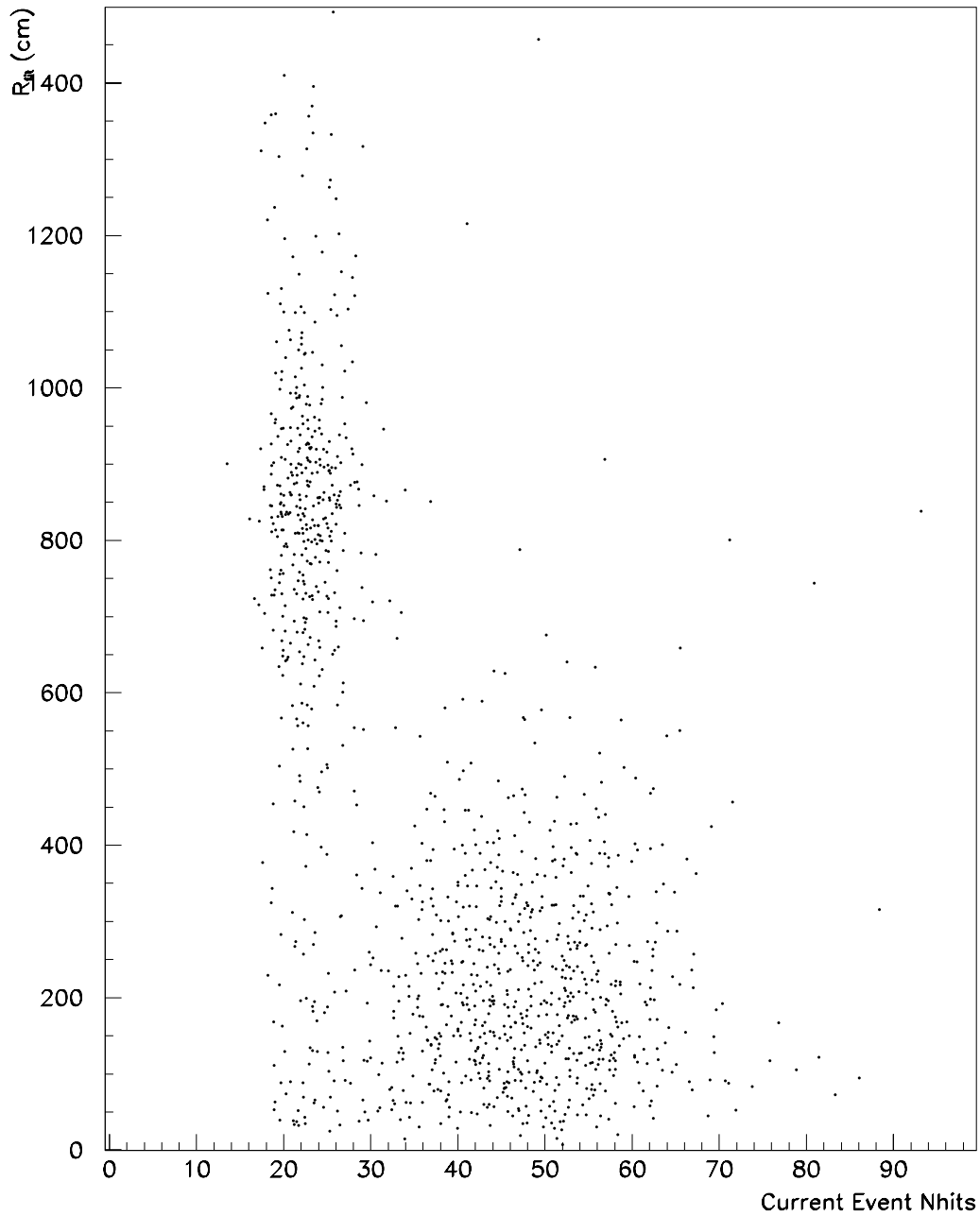


Figure 7: Comparing the  $R_{fit0}$  with  $N_{hits_0}$  shows that most of the low energy events are reconstructed to the radius of the PMT Support Structure ( $\sim 9$  meters). The more diffuse group of data points between 35 and 60 Nhits are, for the most part, neutron events from neutron-neutron coincidence. Data from Runs 11840 and 11841 are included in this plot.

respectively). Though we did not expect the Burst cut to effect the sample since the rate of the calibration source was relatively slow, it was possible that the Burst cut would remove events due to multiple neutrons which happened to capture on D<sub>2</sub>O with very short time separations.

Three other cuts were removed before applying the data cleaning mask. The QBC, QBC2 and QTC cuts all rely on the HQCF bad channel list. When the ntuples used in this analysis were processed, the HQCF list was not used. As a result, had these three cuts been included when the data cleaning was applied, a large number of good neutron events ( $\sim \frac{1}{2}$  of the sample) would have been removed.

Figure 8 shows three Nhits<sub>0</sub> distributions: without the data cleaning, with the data cleaning including the Burst cut and with the data cleaning not including the Burst cut. All of the distributions include a 30 Nhit<sub>1</sub> threshold and 4 meter R<sub>fit0,1</sub> cuts. With the exception of two events in the 30-60 Nhit range and 4 events in the 20-25 Nhit range, the data cleaning did not remove any more events than had already been removed by the Nhits and R<sub>fit</sub> cuts. Each histogram in Figure 8 is fit to a gaussian, all of which have a peak at about 47 Nhits. As expected, there is no difference between the histograms with and without the Burst cut. It is interesting to note that the small lower Nhit peak was not significantly affected by the application of the data cleaning. This implies that the events in that peak are good events, in general, though they are not neutron events, based on their Nhits values, and therefore they still need to be removed to obtain a pure neutron sample.

## 5.2 $\Delta t$ of the Purified Sample

Though the event time separation,  $\Delta t$ , was not used in the sample purification, we did use it to check the purified sample (i.e. the neutron sample obtained using the Nhits<sub>1</sub> > 30 and R<sub>fit0,1</sub> < 4m cuts) to determine if it met the expectations for uncorrelated neutron capture. The expected time constant for the exponential decay of  $\Delta t$  is related to the neutron thermalization time in the D<sub>2</sub>O, and is approximately 0.035 seconds. Figure 9 shows the  $\Delta t$  distributions for the purified neutron sample from Runs 11840 and 11841. The time constant is slightly shorter than the expected value. However, considering the low statistics available even using both calibration runs, it is not unreasonable. This implies that it is likely that the sample is composed, for the most part, of neutron events from neutron-neutron coincidence.

## 6 Conclusions

Using neutron-neutron coincidence, it is possible to select a pure neutron sample from <sup>252</sup>Cf. With a combination of Nhits<sub>0-5</sub> and R<sub>fit0-5</sub> cuts, the low energy  $\gamma$  and  $\beta\gamma$  background events can be filtered from the data, leaving the sample of mostly neutrons from neutron-neutron event pairs. This can be verified by looking at the decay constant of the  $\Delta t$  distribution. Further work is needed to determine the most efficient combination of Nhits and R<sub>fit</sub> cuts, and to evaluate the systematic uncertainties and efficiencies for all of the cuts applied in the neutron selection procedure. Additionally, it will be important to study the possibility

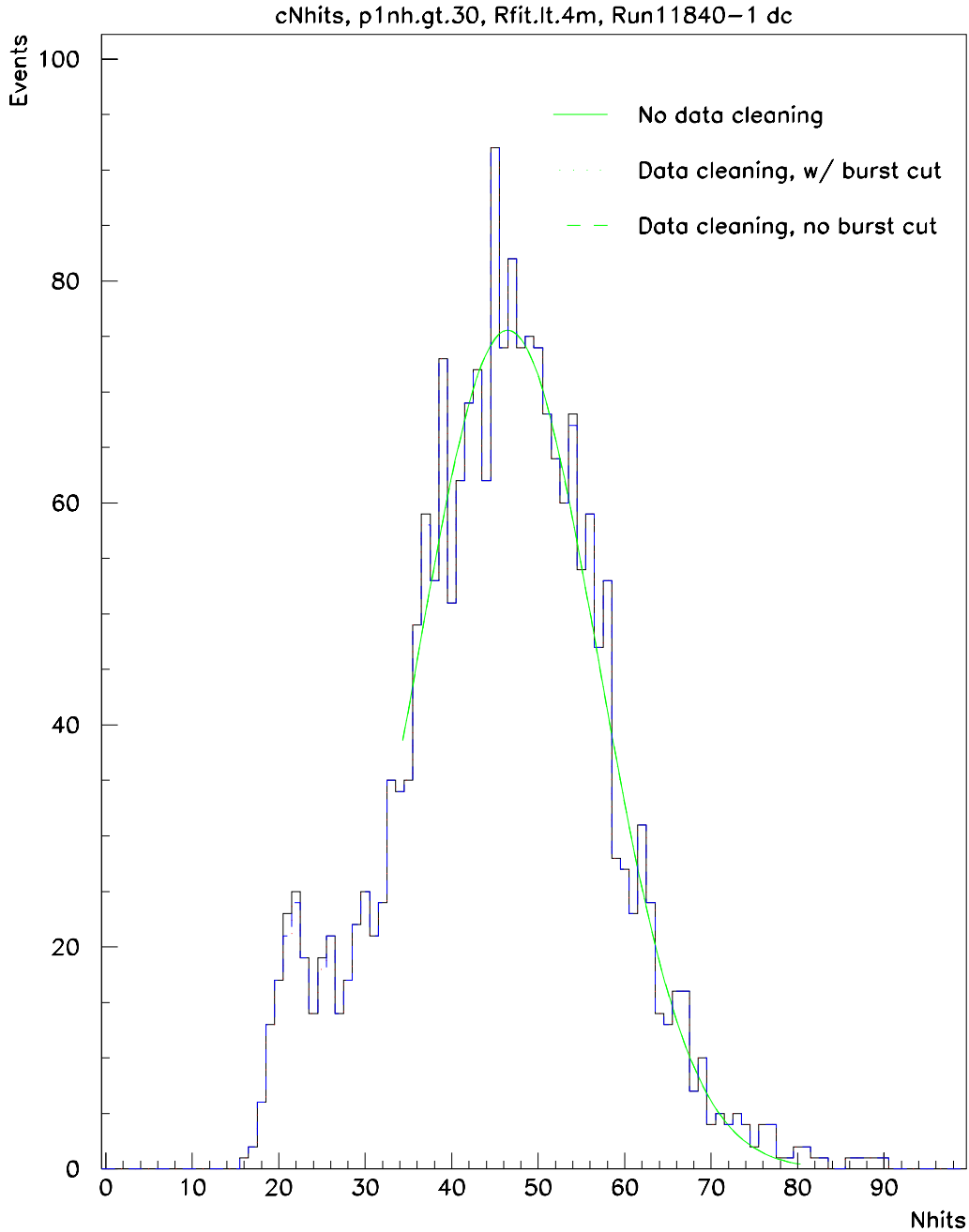


Figure 8: These histograms show the  $N_{\text{hits}_0}$  spectra with and without data cleaning applied. Of the two histograms for which the data cleaning was applied, one includes the Burst cut, and the other does not. The DARN masks used were 0xB3B07 and 0xB3B06, respectively. The other cuts used to create these plots are  $N_{\text{hits}_1} > 30$  and  $R_{\text{fit},0,1} < 4m$ . These plots include data from Runs 11840 and 11841.

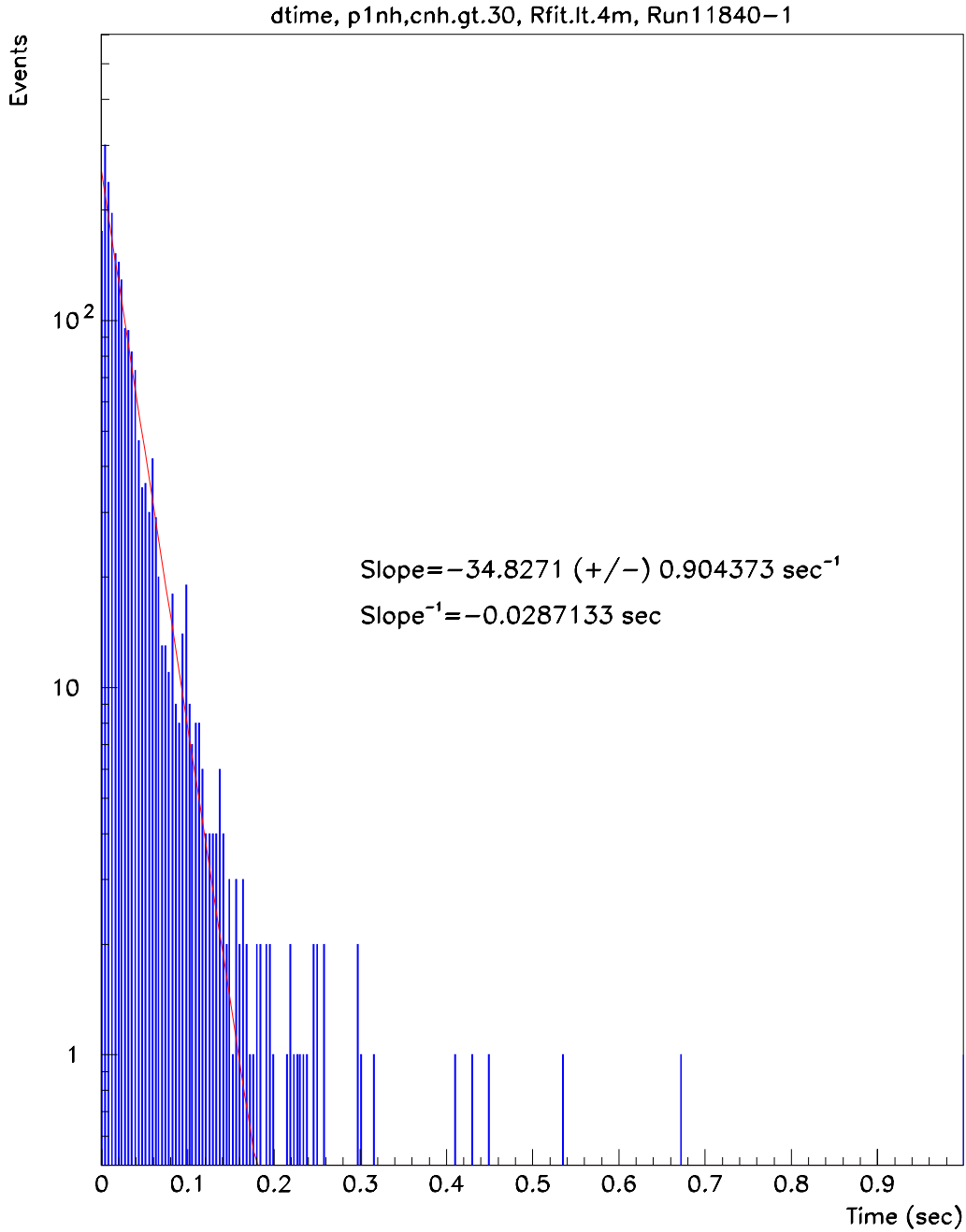


Figure 9: The distribution of the event pair time separation,  $\Delta t$ , decays exponentially, as would be expected for uncorrelated pairs of neutron capture. The decay constant of this plot is close to, but slightly short of the expected value,  $\sim 0.035$  seconds. Runs 11840 and 11841 were used to create this histogram.

of using  $\Delta t$  as the next step in the neutron selection. The SNO collaboration may add a scintillator disc in the calibration source to enhance the signal of the low energy  $\gamma$  rays from the  $^{252}\text{Cf}$  spontaneous fission. Then the same coincidence technique can be applied to looking for  $\gamma$ -neutron coincidence.

## 7 Acknowledgements

I thank the United States Department of Energy – Office of Science for giving me the opportunity to participate in the Energy Research Undergraduate Laboratory Fellowship program.

My thanks also go to my mentors, Kevin Lesko, Alan Poon, Colin Okada and the entire SNO group at Lawrence Berkeley National Laboratory. I also thank the SNO collaboration.

This research was conducted at the Institute for Nuclear and Particle Astrophysics, in the Nuclear Sciences Division at Lawrence Berkeley National Laboratory.